Chinese Journal of Natural Medicines

Isoimperatorin regulates hepatic fibrosis through LXR α / β –HMGB1/NLRP3 axis: insights into the apoptosis of activated hepatic stellate cells in hepatic microenvironment

Saihu Liu, Meiyan Xuan, Chong Gao, Chenyu Wang, Lihua Lian, Jixing Nan, Zhenyu Cui, Yanling Wu

Citation: Saihu Liu, Meiyan Xuan, Chong Gao, Chenyu Wang, Lihua Lian, Jixing Nan, Zhenyu Cui, Yanling Wu, Isoimperatorin regulates hepatic fibrosis through LXR α / β –HMGB1/NLRP3 axis: insights into the apoptosis of activated hepatic stellate cells in hepatic microenvironment, Chinese Journal of Natural Medicines, 2026, 24(11), 1366–1378. doi: 10.1016/S1875–5364(26)61226–5.

View online: https://doi.org/10.1016/S1875–5364(26)61226–5

Related articles that may interest you

Picroside II promotes HSC apoptosis and inhibits the cholestatic liver fibrosis in Mdr2$^{/}$ mice by polarizing M1 macrophages and balancing immune responses

Chinese Journal of Natural Medicines. 2024, 22(7), 582–598 https://doi.org/10.1016/S1875–5364(24)60571–6

β –Elemene induces apoptosis and autophagy in colorectal cancer cells through regulating the ROS/AMPK/mTOR pathway

Chinese Journal of Natural Medicines. 2022, 20(1), 9–21 https://doi.org/10.1016/S1875–5364(21)60118–8

Yanggan Jiangmei Formula alleviates hepatic inflammation and lipid accumulation in non–alcoholic steatohepatitis by inhibiting the NF– κ B/NLRP3 signaling pathway

Chinese Journal of Natural Medicines. 2024, 22(3), 224–234 https://doi.org/10.1016/S1875–5364(24)60595–9

Ligustroflavone ameliorates CCl_4–induced liver fibrosis through down–regulating the TGF– β /Smad signaling pathway

Chinese Journal of Natural Medicines. 2021, 19(3), 170–180 https://doi.org/10.1016/S1875–5364(21)60018–3

Qi–Tai–Suan, an oleanolic acid derivative, ameliorates ischemic heart failure *via* suppression of cardiac apoptosis, inflammation and fibrosis

Chinese Journal of Natural Medicines. 2022, 20(6), 432–442 https://doi.org/10.1016/S1875–5364(22)60156–0

Anti–hepatitis B virus activities of natural products and their antiviral mechanisms

Chinese Journal of Natural Medicines. 2023, 21(11), 803–811 https://doi.org/10.1016/S1875–5364(23)60505–9

Wechat

Chinese Journal of Natural Medicines 24 (2026) 1366-1378

Contents lists available at ScienceDirect

Chinese Journal of Natural Medicines

journal homepage: www.cjnmcpu.com/



Original article

Isoimperatorin regulates hepatic fibrosis through LXRα/β-HMGB1/NLRP3 axis: insights into the apoptosis of activated hepatic stellate cells in hepatic microenvironment

Saihu Liu[a], Meiyan Xuan[b], Chong Gao[a], Chenyu Wang[a], Lihua Lian[a], Jixing Nan[a,*], Zhenyu Cui[a,*], Yanling Wu[a,*]

[a] *Key Laboratory for Traditional Chinese Korean Medicine Research (State Ethnic Affairs), College of Pharmacy, Yanbian University, Yanji 133002, China*
[b] *School of Pharmaceutical Sciences, Josai University, Saitama 330-9301, Japan*

ARTICLE INFO

Article history:
Received 3 February 2026
Revised 12 July 2026
Accepted 16 August 2026
Available online 20 November 2026

Keywords:
Isoimperatorin
Hepatic fibrosis
Hepatic microenvironment
LXRα/β
HMGB1-NLRP3
Apoptosis

ABSTRACT

Hepatic fibrosis is a pathological response to persistent liver injury, characterized by activation of hepatic stellate cells (HSCs) and excessive extracellular matrix (ECM) deposition. Isoimperatorin (ISOIM), a coumarin derivative isolated from *Angelica dahurica*, has been reported to possess analgesic and anti-inflammatory properties. This study investigated the hepatoprotective potential of ISOIM and its underlying mechanisms against hepatic fibrosis. C57BL/6J mice were intraperitoneally injected with thioacetamide (TAA, 100–200 mg·kg^{-1}) for 5 weeks and received ISOIM (5 or 8 mg·kg^{-1}) administration. HSCs and LX-2 were stimulated with transforming growth factor-β (TGF-β, 10 nmol·L^{-1}) or conditioned medium from lipopolysaccharide (LPS)-primed THP-1 (LPS-MØ-CM), followed by ISOIM (0.78, 1.56, 3.125 μmol·L^{-1}) treatment. In TAA-induced mice, ISOIM reduced serum transaminases, attenuated ECM deposition and histopathological damage, alleviated inflammatory responses, and decreased hepatocyte apoptosis. In activated HSCs, ISOIM inhibited ECM accumulation, reduced inflammatory cytokine expression and promoted apoptotic signaling. Mechanistically, ISOIM showed a potential interaction with LXRα/β, reduced HMGB1-associated inflammatory signaling, and suppressed activation of the HMGB1/NLRP3 signaling, accompanied by enhanced caspase-3-mediated apoptotic signaling in activated HSCs. These effects were consistent with those of the LXRα/β agonist GW3965 and were markedly attenuated by LXRβ or LXRα silencing. In addition, ISOIM regulated LXRα/β and the HMGB1-NLRP3 axis, reduced α-SMA expression, and promoted apoptotic signaling in LX-2 cultured with LPS-MØ-CM. Collectively, ISOIM exerted hepatoprotective effects by activating LXRα/β, inhibiting HMGB1/NLRP3 signaling, and promoting apoptosis of activated HSCs within the hepatic microenvironment.

1. Introduction

Hepatic fibrosis is a progressive pathological process arising from persistent liver injury caused by various etiologies, including viral infection, excessive alcohol consumption, autoimmune disorders, and exposure to hepatotoxic chemicals [1]. It is characterized by chronic inflammation, activation of hepatic stellate cells (HSCs), and dysregulated extracellular matrix (ECM) remodeling, ultimately leading to architectural distortion of liver lobules and hepatic microenvironment remodeling [2, 3]. Although early-stage fibrosis can regress upon removal of the noxious stimulus, sustained parenchymal injury frequently progresses to irreversible cirrhosis and hepatocellular carcinoma [4]. However, effective clinical therapeutic options for hepatic fibrosis remain limited, and there remains an urgent need to develop anti-fibrotic agents [5]. Activated HSCs are the major effector cells responsible for excessive ECM deposition, and their clearance, including apoptosis of activated HSCs, is considered an important mechanism contributing to fibrosis resolution [6]. Therefore, elucidating the cellular and molecular mechanisms that regulate HSCs activation, survival, and apoptosis remains crucial for developing effective strategies to prevent or attenuate hepatic fibrosis.

During chronic liver injury, HSCs activation is not only driven by direct fibrogenic stimulation, but is also profoundly shaped by signals derived from neighboring parenchymal and immune cells within the hepatic microenvironment [7]. Injured and apoptotic hepatocytes contribute to the release of damage-associated molecular patterns (DAMPs), among which high mobility group box 1 (HMGB1) is a representative pro-inflammatory mediator [8]. These danger signals recruit and activate inflammatory cells, particularly hepatic macrophages, thereby disrupting hepatic microenvironmental homeostasis and further promoting HSCs activation [9]. In this inflammatory context, activation of the NOD-like receptor family pyrin domain-containing 3 (NLRP3) inflammasome may promote inflammatory mediator maturation, including interleukin-1β (IL-1β) and interleukin-18 (IL-18), and may amplify NLRP3 signaling-associated inflammatory responses under certain pathological conditions [10]. NLRP3 inflammasome ac-

* Corresponding author.
E-mail addresses: ylwu@ybu.edu.cn (YL. Wu); cuizhenyu@ybu.edu.cn (ZY. Cui); jxnan@ybu.edu.cn (JX. Nan)

https://doi.org/10.1016/S1875-5364(26)61226-5
Copyright © 2026, China Pharmaceutical University. Published by Elsevier B.V. All rights are reserved.

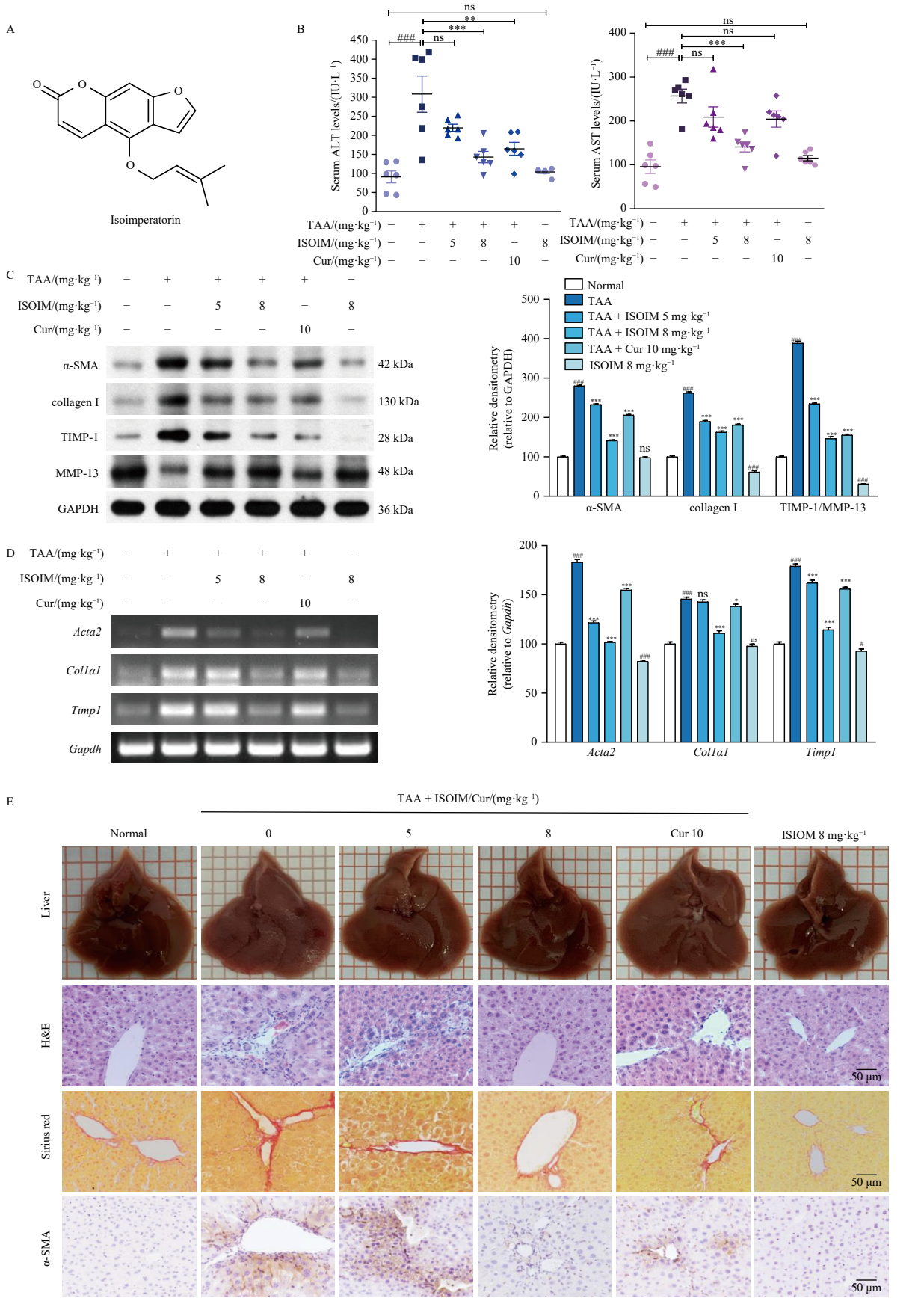


Fig. 1 ISOIM protected against liver injury and ECM accumulation in TAA-induced mice. (A) Chemical structure of ISOIM. (B) Serum ALT and AST levels (n = 6) in TAA-induced mice treated with ISOIM or Cur. (C) Representative western blotting analysis of α-SMA, collagen I, TIMP-1 and MMP-13 in liver tissues of TAA-induced mice. (D) RT-PCR analysis for expressions of *Acta2*, *Col1α1*, and *Timp1* in liver tissues of TAA-induced mice. (E) Representative histological images of liver appearance, liver sections with H&E staining, Sirius red staining, and immunohistochemical staining for α-SMA (400 × magnification, scale bar = 50 μm) in TAA-induced mice. Protein and mRNA expressions were quantified relative to GAPDH as an internal control. Data were presented as mean ± SD (n = 3). Statistical significance was determined by one-way ANOVA with Tukey's post-hoc test. $^{\#}P < 0.05$, $^{\#\#\#}P < 0.001$ *vs* normal group; $^{*}P < 0.05$, $^{***}P < 0.001$ *vs* TAA group; ns, no significant difference.

tivation in HSCs may amplify local inflammation, reinforce communication between macrophages and HSCs, and aggravate ECM deposition, thereby contributing to the progression of hepatic fibrosis [11]. Therefore, regulation of HMGB1/NLRP3 signaling may represent an important mechanism for modulating HSCs fate and fibrogenic progression within the hepatic microenvironment.

Nuclear receptors have attracted increasing attention as pharmacological targets for regulating hepatic inflammation, metabolic disturbance, and fibrogenic remodeling [12-14]. Among them, liver X receptors (LXRs), including liver X receptor alpha (LXRα) and liver X receptor beta (LXRβ), are ligand-activated transcription factors that maintain lipid homeostasis by regulating cholesterol efflux, fatty acid metabolism, and phospholipid remodeling [15, 16]. Beyond their metabolic functions, LXRs have also been recognized as important negative regulators of inflammatory responses [17]. Activation of LXRs signaling has been reported to suppress macrophage-mediated cytokine production, restrain NLRP3 inflammasome-associated inflammatory cascades, and alleviate liver injury under pathological conditions [18]. Conversely, impaired LXRs signaling is associated with aggravated hepatic inflammation, enhanced HSCs activation, and fibrogenic progression [19]. These findings suggest that pharmacological modulation of LXRs may represent a promising strategy for improving hepatic microenvironment, restraining inflammation-driven injury, and attenuating hepatic fibrosis.

Traditional Chinese medicines demonstrate multi-target therapeutic potential and low toxicity in the treatment of hepatic injury and fibrosis, with *Angelica dahurica* possessing multiple pharmacological effects, including analgesic, anti-inflammatory, hepatoprotective, and anti-hyperlipidemic properties [20]. Our previous study found that *Angelica dahurica* extract exerted protective effects against carbon tetrachloride (CCl_4)-induced liver injury [21]. Isoimperatorin (ISOIM), a major bioactive coumarin isolated from *Angelica dahurica*, has also shown favorable liver distribution and anti-inflammatory pharmacological activity [22]. In addition, ISOIM preferentially accumulates in the liver and upregulates heme oxygenase-1 (HO-1) expression in hepatocytes, thereby contributing to the defense against oxidative stress [23, 24]. ISOIM can induce cell cycle arrest and promote apoptosis in hepatocellular carcinoma cells [25]. These findings suggest that ISOIM has potential relevance to liver protection and apoptotic signaling regulation.

Therefore, the present study aimed to investigate the protective effect of ISOIM against hepatic fibrosis and associated inflammation in thioacetamide (TAA)-induced mice and activated HSCs. Specifically, we examined whether ISOIM promotes apoptosis of activated HSCs while suppressing HMGB1/NLRP3 signaling through modulation of LXRα/β within the hepatic microenvironment. We further examined the involvement of crosstalk between macrophages and HSCs in this process, aiming to provide mechanistic evidence for ISOIM as a potential natural product-derived candidate for anti-fibrotic intervention.

2. Materials and methods

2.1. Materials and reagents

ISOIM (CAS No.:482-45-1; Molecular Formula: $C_{16}H_{14}O_4$; Fig. 1A; purity > 97%) was supplied by Derick Biotechnology Co., Ltd. (Chengdu, China). Primary antibodies against glyceraldehyde-3-phosphate dehydrogenase (GAPDH; ab8245), tissue inhibitor of metalloproteinase-1 (TIMP-1; ab61224), matrix metalloproteinase-13 (MMP-13; ab75606), HMGB1 (ab79823), NLRP3 (ab4207), myeloperoxidase (MPO; ab45977), and F4/80 (ab6640) were obtained from Abcam (Cambridge, MA, USA). Primary antibodies against alpha-smooth muscle actin (α-SMA; bs10196R) and Type I collagen (collagen I; bs0578R) were obtained from Bioss Antibodies (Beijing, China). Primary antibodies against LXRα/β (sc-377260), apoptosis-associated speck-like protein containing a caspase recruitment domain (ASC; sc-514414), cysteine-aspartic protease-1 (caspase-1; sc-5140), B-cell lymphoma 2 (Bcl-2; sc-7382), Bcl-2-associated X protein (Bax; sc-7480), cysteine-aspartic protease-3 (caspase-3; sc-56053), and interleukin-1 receptor type 1 (IL1R1; sc-393998) were purchased from Santa Cruz Biotechnology Inc. (Santa Cruz, CA, USA). Anti-IL-1β (AF-401NA) was purchased from R&D Systems (Minneapolis, MN, USA). Primary antibody against gasdermin D (GSDMD; AF4012) was obtained from Affinity Biosciences (Cincinnati, OH, USA). Anti-IL-18 (K110408P), dimethyl sulfoxide (DMSO), and radioimmunoprecipitation assay (RIPA) buffer were purchased from Solarbio (Beijing, China). Dulbecco's modified Eagle medium (DMEM) was purchased from Sigma-Aldrich (St. Louis, MO, USA). Fetal bovine serum (FBS) was purchased from Gibco (Grand Island, NY, USA). The immunohistochemistry kit was purchased from Maixin-Bio (Fuzhou, China).

2.2. Animal procedures and treatments

Male C57BL/6 mice (6–8 weeks old, body weight 20 ± 2 g) were provided by the Changchun Yisi Laboratory Animal Technology Co., Ltd. (Jilin, China). All mice were housed in a specific pathogen-free (SPF) facility under standard environmental conditions (25 °C, 12 h/12 h light/dark cycle) with free access to water and food. All animals received humane care in accordance with the U.K. Animals (Scientific Procedures) Act, 1986 and associated guidelines. All experiments complied with the ARRIVE guidelines and were approved by the Institutional Animal Ethics Care and Use Committee of Yanbian University (Ethical Approval No. YD20250122009).

All mice were randomly assigned into 6 groups (n = 6): normal group, TAA group, TAA + ISOIM (5 or 8 mg·kg^{-1}) groups, TAA + curcumin (Cur, 10 mg·kg^{-1}) group and ISOIM single administration (8 mg·kg^{-1}) group, using simple unrestricted randomization. The dosages of ISOIM were selected according to our previous experiments and other studies [20, 21, 26]. TAA (100 mg·kg^{-1}) was injected intraperitoneally 3 times in 1st week, and TAA (200 mg·kg^{-1}) was injected twice *per* week from 2nd to 5th weeks to induce hepatic fibrosis. Mice in ISOIM or Cur groups were administered ISOIM (5 or 8 mg·kg^{-1}) or Cur (10 mg·kg^{-1}) by gavage daily from 2nd to 5th week. Mice in normal group were given an equal volume of saline. Six hours after the last administration, the mice were euthanized after anesthetization with an intraperitoneal injection of pentobarbital sodium (1%, 50 mg·kg^{-1}). The serum and liver tissues were collected for subsequent experimental analysis.

2.3. Serum biochemical analysis

After blood collection from mice, the samples were centrifuged to obtain serum. Serum alanine aminotransferase (ALT) and aspartate aminotransferase (AST) levels were measured according to the manufacturer's instructions using commercial kits purchased from Changchun Huili Bioengineering Institute (Changchun, China).

2.4. Histopathological analysis

Liver tissues were fixed in 10% formalin, embedded in paraffin, and cut into 5-μm sections. The liver sections were subjected to hematoxylin and eosin (H&E) staining, Sirius Red staining, and immunohistochemical staining, and then observed under a light microscope (Nikon, Japan).

2.5. Network pharmacology analysis and molecular docking

Potential targets of ISOIM were obtained from TCMSP and

STITCH databases, and STITCH targets with a confidence score > 0.7 were retained. Hepatic fibrosis-related targets were collected from OMIM, GeneCards, and DisGeNET databases. The overlapping targets were subjected to protein-protein interaction (PPI) analysis using STRING and visualized using Cytoscape v3.10.0. Core targets were identified based on node degree. Gene Ontology (GO) and Kyoto Encyclopedia of Genes and Genomes (KEGG) enrichment analyses were performed using DAVID.

The chemical structure of ISOIM was obtained from PubChem, and the structures of target proteins were obtained from the RCSB Protein Data Bank. After structural preprocessing using PyMOL 2.6.0, molecular docking was performed using AutoDock Vina 1.1.2. Docking results were evaluated based on binding affinity and visualized using PyMOL.

2.6. Cell culture and treatment

HSC-T6 (rat hepatic stellate cell line, CVCL_0315), LX-2 (human hepatic stellate cell line, CVCL_5792) and the THP-1 cell line (immortalized human monocytic-leukemia cells, CVCL_0006) were generously provided by Professor Jung Joon Lee (Korea Institute of Bioscience and Biotechnology, Daejeon, Korea). Cells (passage ranging from 3 to 10) were cultured in DMEM or Roswell Park Memorial Institute 1640 medium (RPMI-1640) supplemented with 10% FBS, 100 U·mL^{-1} penicillin and 100 μg·mL^{-1} streptomycin, under the conditions of 5% CO_2 and 37 °C.

HSC-T6 was stimulated by transforming growth factor-β (TGF-β, 10 nmol·L^{-1}), then was treated with ISOIM (0.78, 1.56, 3.125 μmol·L^{-1}), GW3965 (1 μmol·L^{-1}) or SR9243 (10 μmol·L^{-1}). THP-1 was differentiated into macrophages by using phorbol ester (PMA, 100 nmol·L^{-1}), then exposed to lipopolysaccharide (LPS, 1 μg·mL^{-1}) for 4 h. Conditioned medium from LPS-primed THP-1 (LPS-MØ-CM) was collected and applied to LX-2 with or without ISOIM (3.125 μmol·L^{-1}).

2.7. Cell viability assay

HSC-T6 or AML12 was incubated with ISOIM (0−100 μmol·L^{-1}) for 24 h. Subsequently, 3-(4, 5-Dimethylthiazol-2-yl)-2, 5-diphenyltetrazolium bromide (MTT) was added, and the formazan crystals were dissolved in DMSO. The absorbance was measured at 570 nm using a multi-mode microplate reader (BioTek Synergy HTX, VT, USA).

2.8. Co-immunoprecipitation assay (Co-IP assay)

Co-IP assay was performed to detect the interaction among LXRβ, HMGB1, and NLRP3. Briefly, cell lysates were precleared and then incubated with anti-HMGB1 antibody or IgG as a negative control. The immune complexes were captured using protein A/G agarose beads according to the manufacturer's instructions. The precipitated proteins were then subjected to western blotting analysis.

2.9. Small interfering RNA transfection

LX-2 was transfected with negative control small interfering RNA (sicontrol), LXRβ-targeting siRNA (siLXRβ) and LXRα-targeting siRNA (siLXRα) using Lipofectamine RNAiMAX (Thermo Fisher Scientific Inc., Waltham, MA, USA) according to the manufacturer's instructions.

2.10. Apoptosis staining

The culture medium of cells was replaced with DMEM containing Annexin V-mCherry and SYTOX Green at the recommended working concentrations. Apoptotic cells were observed by fluorescence microscopy, and the apoptotic rate was quantified by flow cytometry.

2.11. Immunofluorescence staining assay

Cultured cells or frozen sections were fixed with 4% paraformaldehyde, permeabilized with 0.1% Triton X-100, and blocked with 5% goat serum. The samples were incubated with primary antibodies, followed by incubation with secondary antibodies. Finally, nuclei were counterstained with aqueous Fluoroshield mounting medium containing 4′,6-diamidino-2-phenylindole (DAPI).

2.12. Western blotting experiment

Total protein was extracted from cells and liver tissues using RIPA lysis buffer. Briefly, protein concentrations were determined using a bicinchoninic acid (BCA) protein assay kit (Beyotime, China). Equal amounts of protein samples were separated by sodium dodecyl sulfate-polyacrylamide gel electrophoresis (SDS-PAGE) and transferred onto polyvinylidene difluoride (PVDF) membranes. The membranes were blocked and incubated with primary antibodies, followed by incubation with horseradish peroxidase (HRP)-conjugated secondary antibodies. Protein bands were visualized using enhanced chemiluminescence (ECL) reagent (Beyotime, China) and quantified using Quantity One software (Bio-Rad, CA, USA).

2.13. Cellular thermal shift assay (CETSA)

To evaluate the thermal stabilization of LXRα/β by ISOIM, protein concentrations of the cell lysates were determined using a BCA assay, and equal amounts of protein samples were heated in a real-time PCR machine from 37 to 61 °C. After centrifugation, the supernatant was collected and analyzed by western blotting analysis.

2.14. RT-PCR analysis

Total RNA from animals and cells was isolated by using Easteep Super Total RNA Extraction Kit (Promega Biological Products Ltd., Shanghai, China) according to the manufacturer's instructions. The amplified products were separated by agarose gel electrophoresis and visualized with ethidium bromide staining. RT-PCR was performed using the primers listed in Table 1.

2.15. Statistical analysis

All data were expressed as the mean ± SD. The normality of data was tested by the Shapiro-Wilk test and evaluated by a one-way analysis of variance (ANOVA) and Tukey's multiple comparison tests by using GraphPad Prism (GraphPad Software, San Diego, CA, USA). $P < 0.05$ was considered statistically significant.

3. Results

3.1. ISOIM protected against liver injury and ECM accumulation in TAA-induced mice

Serum ALT and AST levels were elevated in TAA group compared with normal group, and were significantly reduced by ISOIM or Cur (Fig. 1B). TAA up-regulated the expressions of α-SMA, collagen I, and TIMP-1, while down-regulating MMP-13 expression. ISOIM or Cur inhibited α-SMA, collagen I, and TIMP-1 expressions, while simultaneously up-regulating MMP-13 expression (Figs. 1C and 1D). Livers from normal mice exhibited a

Table 1 The primer sequences for RT-PCR.

Target	Primer	Primer sequences (5′-3′)
Gapdh	Forward	CTTGTGCAGTGCCAGCC
	Reverse	GCCCAATACGGCCAAATCC
Acta2	Forward	CATCAGGGAGTAATGGTTGG
	Reverse	CACAATACCAGTTGTACGTC
Col1α1	Forward	TGAGTCAGCAGATTGAGAAC
	Reverse	TACTCGAACGGGAATCCATC
Timp1	Forward	GGAAAGCCTCTGTGGATATG
	Reverse	AACAGGAAACACTGTGC
Tnfα	Forward	TCACACTCAGATCATCTTCTC
	Reverse	AGACTCCTCCCAGGTATATG
Il18	Forward	GATCAAAGTGCCAGTGAACC
	Reverse	AACTCCATCTTGTTGTGTCC
Il1b	Forward	GTACATCAGCACCTCACAAG
	Reverse	CACAGGCTCTCTTTGAACAG

smooth surface, whereas TAA caused rough and discolored liver surfaces. ISOIM or Cur markedly improved these gross morphological abnormalities (Fig. 1E). H&E staining revealed extensive hepatocyte degeneration and damage to liver lobules in TAA-induced mice, while these pathological alterations were ameliorated with ISOIM or Cur (Fig. 1E). Sirius Red staining demonstrated marked collagen deposition in liver tissues from TAA group, which was reduced by ISOIM or Cur (Fig. 1E). Immunohistochemical staining also showed enhanced α-SMA-positive staining in TAA-induced mice, which was reduced by ISOIM or Cur (Fig. 1E). Notably, the effects of ISOIM on serum transaminases, fibrotic markers, collagen deposition, and histopathological improvement were generally comparable to those of Cur. These findings suggested that ISOIM exerted hepatoprotective effects by attenuating liver injury and reducing ECM accumulation in hepatic fibrosis.

3.2. ISOIM attenuated immune cell recruitment, cytokine release and hepatocyte apoptosis in TAA-induced mice

TAA significantly up-regulated the mRNA expressions of *Tnfα* and *Il1b* compared with normal mice, which were suppressed with ISOIM or Cur (Fig. 2A). TAA also promoted the expressions of MPO and F4/80 compared with normal group, while ISOIM or Cur inhibited their expressions (Figs. 2B and 2C). TAA also up-regulated the protein expressions of IL1R1, mature-IL-1β and pro-GSDMD compared with normal group, which were reduced by ISOIM (Fig. 2B). Moreover, the Bax/Bcl-2 ratio was significantly enhanced in TAA-induced mice compared with normal group, indicating hepatocyte apoptosis (Fig. 2B). ISOIM or Cur significantly reduced the ratio of Bax/Bcl-2. Notably, ISOIM showed a protective tendency comparable to Cur in suppressing inflammatory gene expression, reducing MPO and F4/80 expression, and lowering the Bax/Bcl-2 ratio. These results suggested that ISOIM effectively inhibited the recruitment of macrophages and neutrophils, reduced the release of inflammatory cytokines, and alleviated hepatocyte apoptosis in TAA-induced mice.

3.3. ISOIM regulated ECM homeostasis and inflammatory responses in activated HSCs

MTT assays showed that ISOIM (6.25–100 μmol·L^{-1}) significantly reduced HSCs viability and ISOIM (25–100 μmol·L^{-1}) significantly reduced AML12 viability (Fig. 3A). Next, ISOIM (0.78, 1.56, 3.125 μmol·L^{-1}) was chosen for subsequent experiments. TGF-β increased the protein and mRNA expressions of α-SMA, collagen I, and TIMP-1 compared with untreated HSCs, while these increases were reduced by ISOIM (Figs. 3B and 3C). The TIMP-1/MMP-13 ratio was also elevated in activated HSCs compared with untreated HSCs, while ISOIM decreased this ratio (Fig. 3C). Immunofluorescence staining further showed that α-SMA-positive staining was enhanced by TGF-β stimulation compared with untreated HSCs and was reduced by ISOIM (Fig. 3D). In addition, ISOIM could significantly reduce the mRNA expressions of *Il18* and *Il1b* in activated HSCs (Fig. 3E). The protein expressions of IL1R1, mature-IL-1β and pro-GSDMD were significantly increased in TGF-β group compared to untreated HSCs, while ISOIM could decrease these inflammatory cytokines expressions (Fig. 3F). Moreover, we found that ISOIM significantly increased the Bax/Bcl-2 ratio compared to TGF-β-stimulated HSCs, which indicated that ISOIM could induce apoptosis of activated HSCs (Fig. 3F). These results suggested that ISOIM reduced excessive ECM accumulation, suppressed inflammatory responses, and promoted apoptotic signaling in activated HSCs.

3.4. ISOIM activated LXRα/β and regulated the HMGB1-NLRP3 pathway in TAA-induced mice

Network pharmacology analysis was performed to preliminarily explore the potential mechanisms of ISOIM against hepatic fibrosis. PPI analysis indicated that the predicted targets were associated with inflammation, apoptosis, and nuclear receptor-related regulation, with caspase-3, NR3C2, and NR1I2 identified as important nodes (Figs. 4A and 4C). KEGG analysis revealed enrichment in apoptosis-, immune-, and metabolism-related pathways (Fig. 4B). GO enrichment analysis showed that these targets were mainly involved in growth factor-related signaling, receptor complex formation, nuclear localization, ATP binding, and protein kinase activity (Fig. 4D). Based on these results and our previous findings, we next examined the effects of ISOIM on LXRα/β expression, NLRP3 inflammasome-related signaling, and caspase-3-associated apoptosis. In this study, LXRα and LXRβ expressions were significantly decreased in TAA-induced mice compared with normal group, which were restored with ISOIM or Cur (Figs. 4E and 4F). TAA also significantly promoted HMGB1, NLRP3, ASC expressions and cleavage of caspase-1 compared with normal group, which were down-regulated by ISOIM or Cur (Figs. 4E and 4F). Notably, ISOIM showed a regulatory tendency comparable to Cur in restoring LXRα/β expression and suppressing HMGB1, NLRP3, ASC expression and caspase-1 cleavage. These findings suggested that ISOIM activated LXRα/β and modulated the HMGB1/NLRP3 inflammasome, thereby alleviating fibrosis and inflammation in TAA-induced mice.

3.5. ISOIM regulated LXRα/β to inhibit HMGB1-NLRP3 signaling and promoted apoptosis in activated HSCs

Molecular docking and CETSA suggested a potential interaction between ISOIM and LXRα/β and indicated increased thermal stability of LXRα/β after ISOIM treatment (Figs. 5A and 5B). In TGF-β-stimulated HSCs, the expressions of LXRα and LXRβ were markedly suppressed, while HMGB1, NLRP3, ASC and caspase-1 expressions were up-regulated. ISOIM treatment restored LXRα and LXRβ expressions, while inhibiting HMGB1, NLRP3 and ASC expressions, and further prevented the cleavage of caspase-1 (Figs. 5C and 5F). In addition, in TGF-β-stimulated HSCs, HMGB1 was predominantly associated with NLRP3 rather than LXRβ. ISOIM treatment appeared to block HMGB1-NLRP3 complex formation, enhancing the binding of HMGB1 to LXRβ (Fig. 5D). Moreover, both MCC950 (an NLRP3 inhibitor) and ISOIM

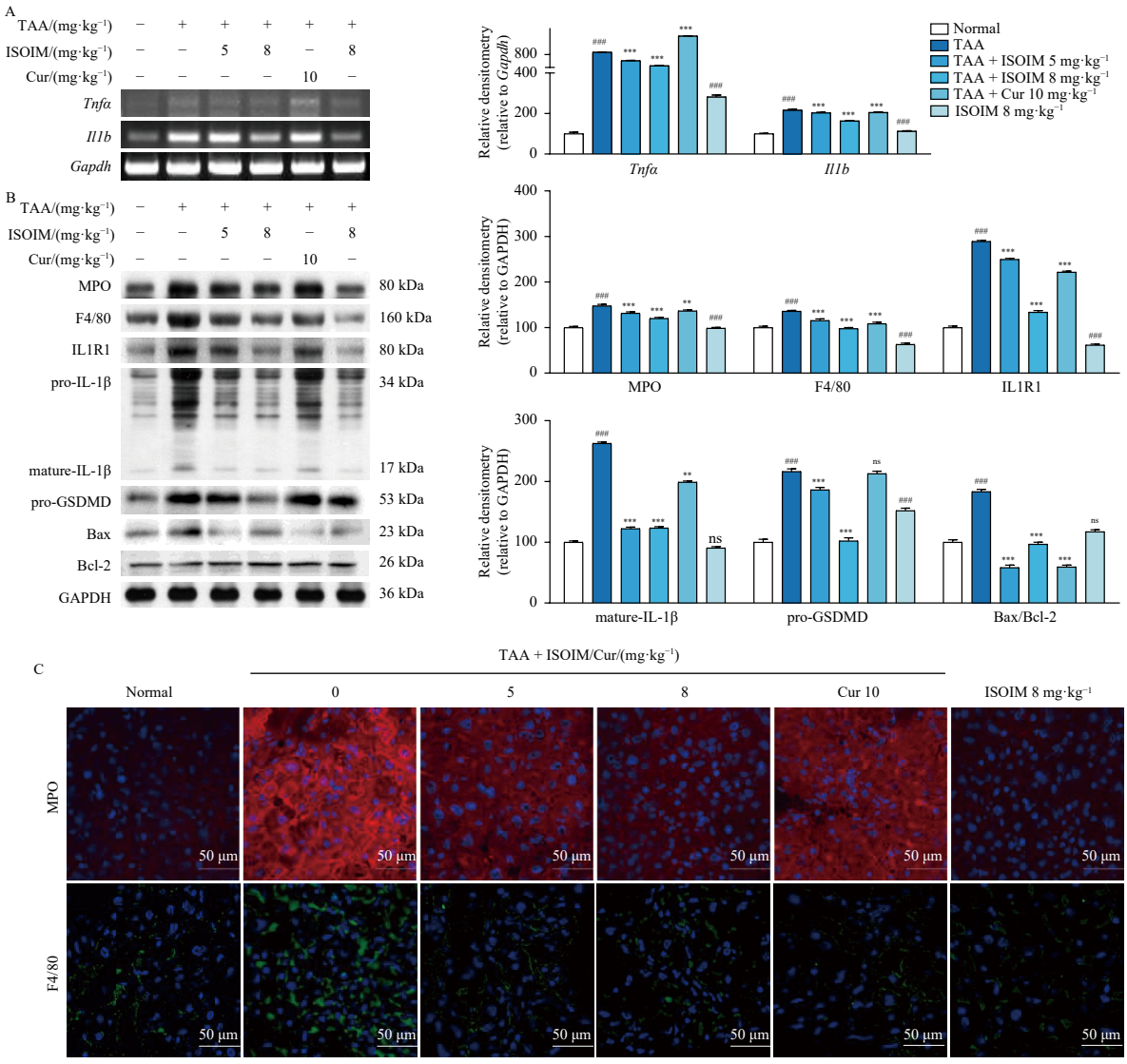


Fig. 2 ISOIM attenuated immune cell recruitment, cytokine release and hepatocyte apoptosis in TAA-induced mice. (A) RT-PCR analysis for expressions of *Tnfα* and *Il1b* in liver tissues of TAA-induced mice. (B) Representative western blotting analysis of MPO, F4/80, IL1R1, pro-IL-1β, mature-IL-1β, pro-GSDMD, Bax and Bcl-2 in liver tissues of TAA-induced mice. (C) Representative histological images of liver sections with immunofluorescence staining for MPO and F4/80 (600 × magnification, scale bar = 50 μm). Protein and mRNA expressions were quantified relative to GAPDH as an internal control. Data were presented as mean ± SD (n = 3). Statistical significance was determined by one-way ANOVA with Tukey's post-hoc test. $^{###}P < 0.001$ *vs* normal group; $^{**}P < 0.01$, $^{***}P < 0.001$ *vs* TAA group; ns, no significant difference.

markedly suppressed NLRP3 expression (Fig. 5F). Interestingly, ISOIM and MCC950 reduced GSDMD cleavage and IL-18 expression, while promoting caspase-3 expression and increasing the Bax/Bcl-2 ratio (Fig. 5E). ISOIM also significantly enhanced the apoptosis of HSCs compared with TGF-β group as shown by SYTOX/Annexin V staining (Fig. 5G). Collectively, these data indicated that ISOIM activated LXRα/β signaling to suppress the HMGB1-NLRP3 signaling, accompanied by reduced GSDMD-N-associated inflammatory signaling and enhanced caspase-3-associated apoptosis in activated HSCs.

3.6. LXRα/β-mediated HMGB1-NLRP3 signaling might be indispensable for the anti-fibrotic effects of ISOIM

In activated HSCs, ISOIM or GW3965 up-regulated LXRβ and LXRα, and further inhibited the expressions of α-SMA, mature-IL-1β, HMGB1, NLRP3, ASC and caspase-1, and enhanced the Bax/Bcl-2 ratio compared to TGF-β group, while SR9243 (an LXRα/β inhibitor) exerted opposite regulatory effects on these protein expressions (Fig. 6A). In addition, immunofluorescence staining also showed that ISOIM or GW3965 enhanced LXRα/β-positive expression, and decreased the positive expressions of α-SMA, HMGB1 and NLRP3 (Fig. 6B). Moreover, LX-2 was cultured with siLXRβ or siLXRα. LXRβ knockdown caused a significant decrease in LXRβ and LXRα, accompanied by up-regulation of α-SMA, mature-IL-1β, GSDMD-N, HMGB1, NLRP3, ASC and cleaved-caspase-1 expressions and down-regulation of the Bax/Bcl-2 ratio compared with sicontrol group, and further inhibited the effects of ISOIM on these proteins (Fig. 6C). Similarly, LXRα knockdown also caused a significant decrease in LXRα and LXRβ, accompanied by up-regulation of α-SMA, mature-IL-1β, GSDMD-N, HMGB1, NLRP3, and cleaved-caspase-1 expressions and down-regulation of the Bax/Bcl-2 ratio compared with sicontrol group, and further attenuated the effects of ISOIM on these proteins (Fig. 6D). These results suggested that ISOIM could inhibit ECM accumulation, HMGB1/NLRP3-mediated inflammation and promote HSCs apoptosis by activating LXRα/β.

3.7. ISOIM modulated the crosstalk of HSCs and macrophages via LXRα/β-mediated HMGB1-NLRP3 axis

Given the significance of the hepatic microenvironment and intercellular communication, we next established a crosstalk model between macrophages and HSCs. Flow cytometry showed that ISOIM significantly increased the proportion of apoptotic LX-2 compared with LPS-MØ-CM group (Fig. 7A). LPS-MØ-CM also

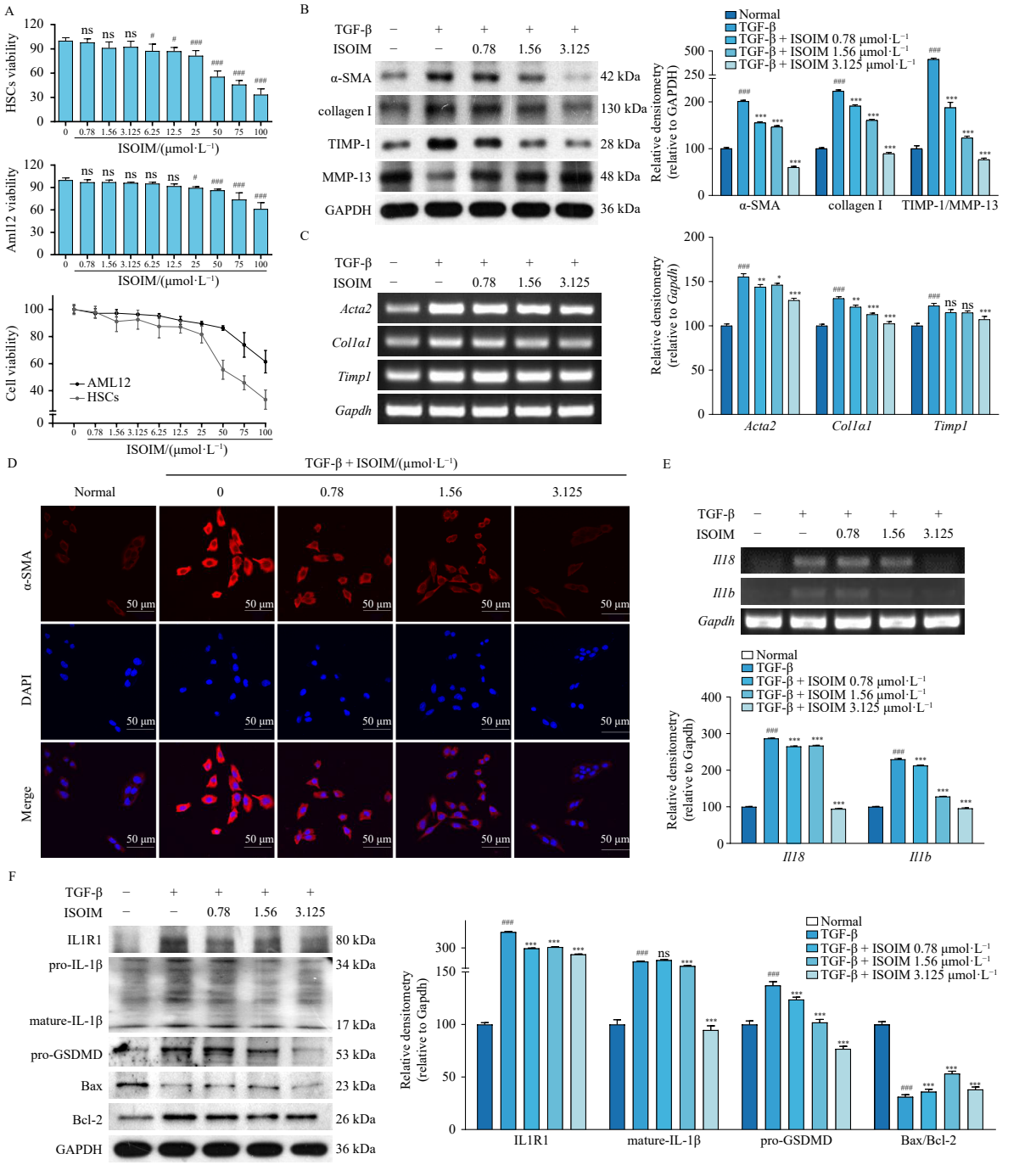


Fig. 3 ISOIM regulated ECM homeostasis and inflammatory response in activated HSCs. (A) MTT assay on cell viability of HSCs and AML12 with ISOIM (0–100 μmol·L^{-1}). (B, F) Representative western blotting analysis of α-SMA, collagen I, TIMP-1, MMP-13, IL1R1, pro-IL-1β, mature-IL-1β, pro-GSDMD, Bax and Bcl-2 in TGF-β-stimulated HSCs. (C, E) RT-PCR analysis for expressions of *Acta2*, *Col1α1*, *Timp1*, *Il18* and *Il1b* in TGF-β-stimulated HSCs. (D) Immunofluorescence staining of α-SMA (600 × magnification, scale bar = 50 μm) in TGF-β-stimulated HSCs. Protein and mRNA expressions were quantified relative to GAPDH as an internal control. Data were presented as mean ± SD (n = 3). Statistical significance was determined by one-way ANOVA with Tukey's post-hoc test. $^{###}P < 0.001$ *vs* untreated HSCs group; $^{*}P < 0.05$, $^{**}P < 0.01$, $^{***}P < 0.001$ *vs* TGF-β group; ns, no significant difference.

increased the protein expressions of α-SMA and mature-IL-1β, and decreased the ratio of Bax/Bcl-2 (Fig. 7B). ISOIM significantly down-regulated α-SMA and mature-IL-1β, and up-regulated the Bax/Bcl-2 ratio (Fig. 7B). These effects were likely due to inhibition of LXRβ and LXRα expressions and promotion of NLRP3 inflammasome assembly by LPS-MØ-CM compared with untreated LX-2 (Fig. 7B). ISOIM significantly increased LXRβ and LXRα expressions, and decreased HMGB1, NLRP3, ASC and cleaved-caspase-1 expressions (Figs. 7B and 7C). Moreover, in LPS-MØ-CM-stimulated LX-2, ISOIM or GW3965 promoted LXRβ and LXRα expressions, and further inhibited the expressions of α-SMA, mature-IL-1β, pro-GSDMD, HMGB1, NLRP3 and caspase-1, and enhanced the Bax/Bcl-2 ratio, in contrast to the effects on these proteins of SR9243 (Fig. 7D). These observations suggested that ISOIM could regulate the crosstalk between macrophages and HSCs through LXRα/β-mediated HMGB1-NLRP3 pathway.

4. Discussion

Although considerable progress has been made in understanding the mechanisms underlying hepatic fibrosis, effective anti-fibrotic drugs remain limited, partly because fibrogenesis is driven by interconnected inflammatory, fibrogenic, and cell death-related pathways [27-31]. In the present study, we demonstrated that ISOIM, a bioactive furanocoumarin derived from *Angelica dahur-*

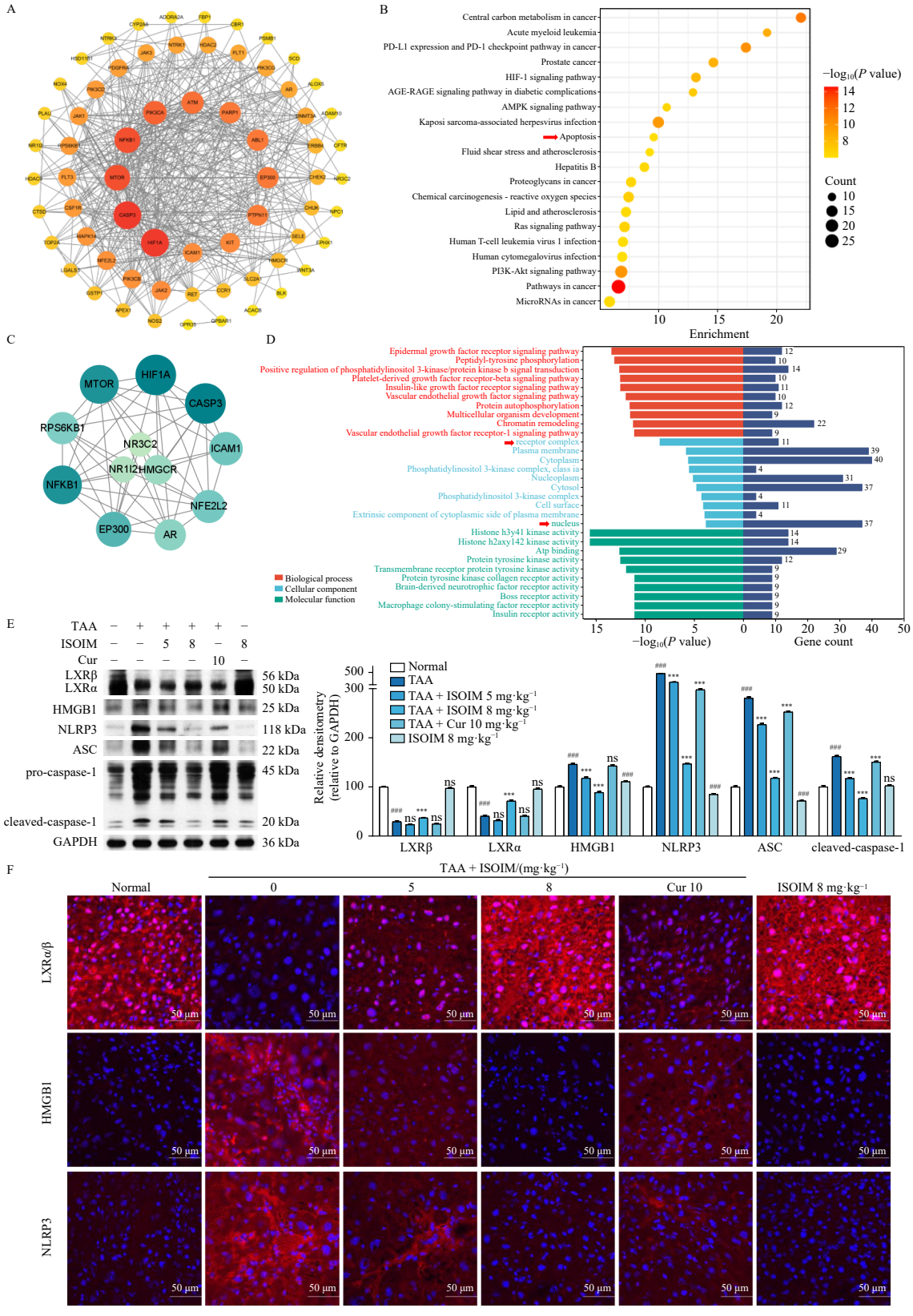


Fig. 4 ISOIM activated LXRα/β and regulated the HMGB1-NLRP3 pathway in TAA-induced mice. (A) ISOIM anti-liver fibrosis PPI network analysis. (B) KEGG pathway enrichment analysis. (C) Second analysis of CytoNCA core network. (D) GO enrichment analysis. (E) Representative western blotting analysis of LXRβ, LXRα, HMGB1, NLRP3, ASC, pro-caspase-1 and cleaved-caspase-1 in liver tissues of TAA-induced mice. (F) Representative histological images of liver sections with immunofluorescence staining for LXRα/β, HMGB1 and NLRP3 (600 × magnification, scale bar = 50 μm). Protein expressions were quantified relative to GAPDH as an internal control. Data were presented as mean ± SD (n = 3). Statistical significance was determined by one-way ANOVA with Tukey's post-hoc test. $^{###}P < 0.001$ *vs* normal group; $^{***}P < 0.001$ *vs* TAA group; ns, no significant difference.

ica, attenuated TAA-induced hepatic fibrosis in mice, as evidenced by decreased ECM deposition, suppressed inflammatory responses, and ameliorated fibrosis-related histopathological changes. Mechanistically, our results suggest that ISOIM exerts anti-fibrotic effects through activation of LXRα/β signaling and subsequent modulation of HMGB1/NLRP3 signaling, accompan-

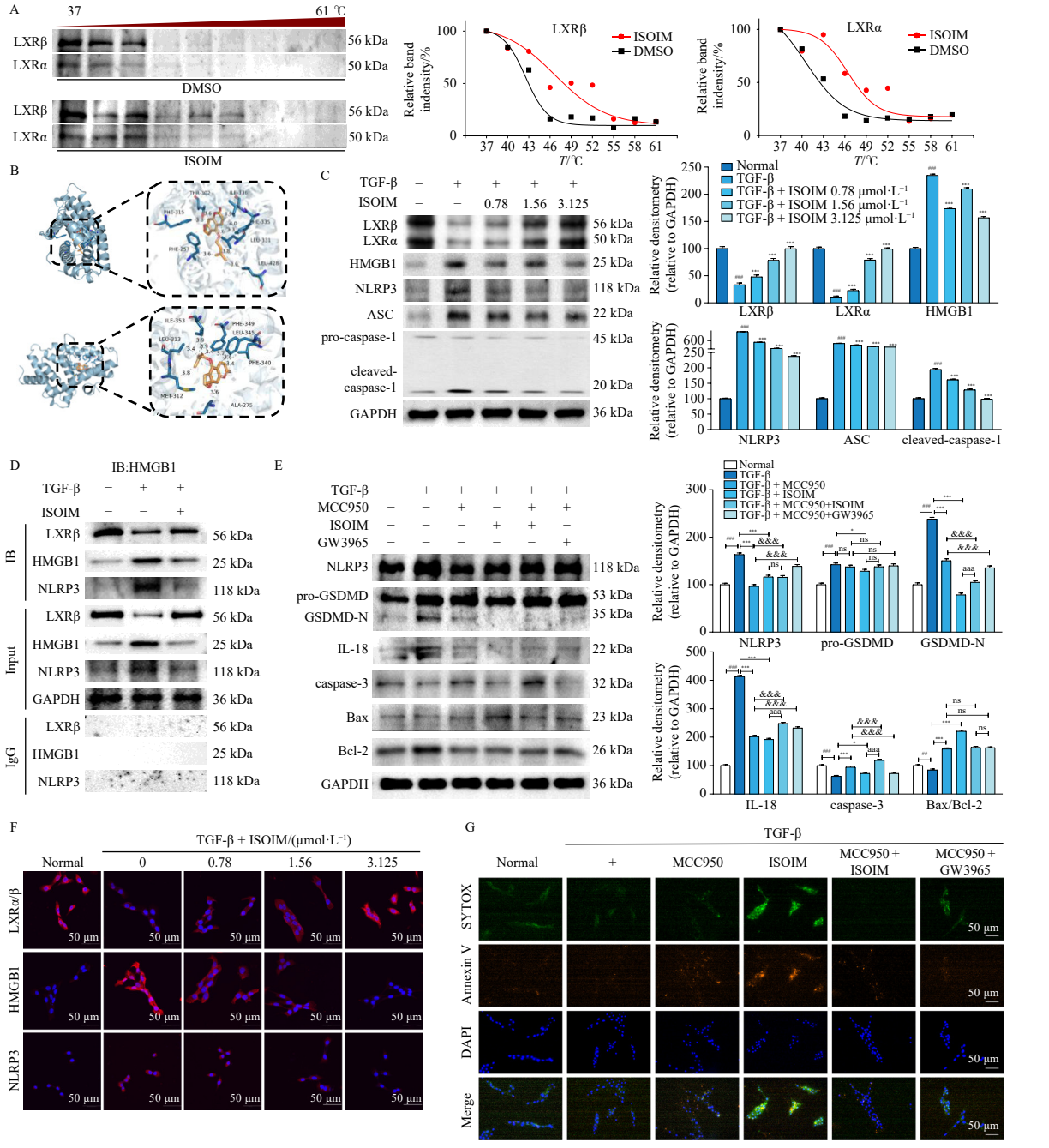


Fig. 5 ISOIM regulated LXRα/β to inhibit HMGB1-NLRP3 axis and promoted apoptosis in activated HSCs. (A) CETSA in ISOIM-treated HSCs. (B) Molecular docking of ISOIM and LXRβ or LXRα. (C) Representative western blotting analysis of LXRβ, LXRα, HMGB1, NLRP3, ASC, pro-caspase-1 and cleaved-caspase-1 in TGF-β-stimulated HSCs. (D) The Co-IP experiment was performed using anti-HMGB1 antibody and then analyzed by representative western blot of LXRβ, HMGB1 and NLRP3. The negative control was IgG. (E) Representative western blotting analysis of NLRP3, pro-GSDMD, IL18, caspase-3, Bax and Bcl-2 in TGF-β-stimulated HSCs. (F) Immunofluorescence staining of LXRα/β, HMGB1 and NLRP3 (600 × magnification, scale bar = 50 μm) in TGF-β-stimulated HSCs. (G) Apoptotic staining (400 × magnification, scale bar = 50 μm) in TGF-β-stimulated HSCs. Protein expressions were quantified relative to GAPDH as an internal control. Data were presented as mean ± SD (n = 3). Statistical significance was determined by one-way ANOVA with Tukey's post-hoc test. $^{\#\#}P < 0.01$, $^{\#\#\#}P < 0.001$ *vs* untreated HSCs group; $^{*}P < 0.05$, $^{***}P < 0.001$ *vs* TGF-β group; $^{\&\&\&}P < 0.001$ *vs* TGF-β + MCC950 group; ns, no significant difference.

ied by reduced downstream inflammatory signaling and enhanced apoptotic signaling.

Promoting apoptosis of activated HSCs has been considered an effective strategy for attenuating hepatic fibrosis, because activated HSCs are the major source of excessive ECM during fibrogenesis [32, 33]. Notably, previous studies using sorafenib and its derivative SC-1 have provided important evidence that induction of apoptosis in activated HSCs can contribute to the attenuation of hepatic fibrosis, supporting the therapeutic relevance of targeting activated HSCs survival in anti-fibrotic intervention [34, 35]. In apoptosis regulation, Bax promotes mitochondrial apoptotic signaling, whereas Bcl-2 counteracts apoptosis by maintaining mitochondrial integrity [36]. In the present study, ISOIM increased caspase-3 activation and elevated the Bax/Bcl-2 ratio in activated HSCs, further supporting its apoptosis-promoting effect. However, the therapeutic application of apoptosis-based anti-fibrotic strategies targeting HSCs remains challenged by the need to selectively eliminate fibrogenic HSCs while minimizing off-target cytotoxicity toward hepatocytes and other non-fibrogenic cells [37, 38]. Our results provided preliminary evidence that ISOIM exhibited differential cytotoxicity toward hepatocytes and HSCs. In addition, administration of ISOIM alone at 8 mg·kg^{-1} did not induce apparent hepatotoxicity *in vivo*, as supported by serum transaminase levels and liver histopathological assessment.

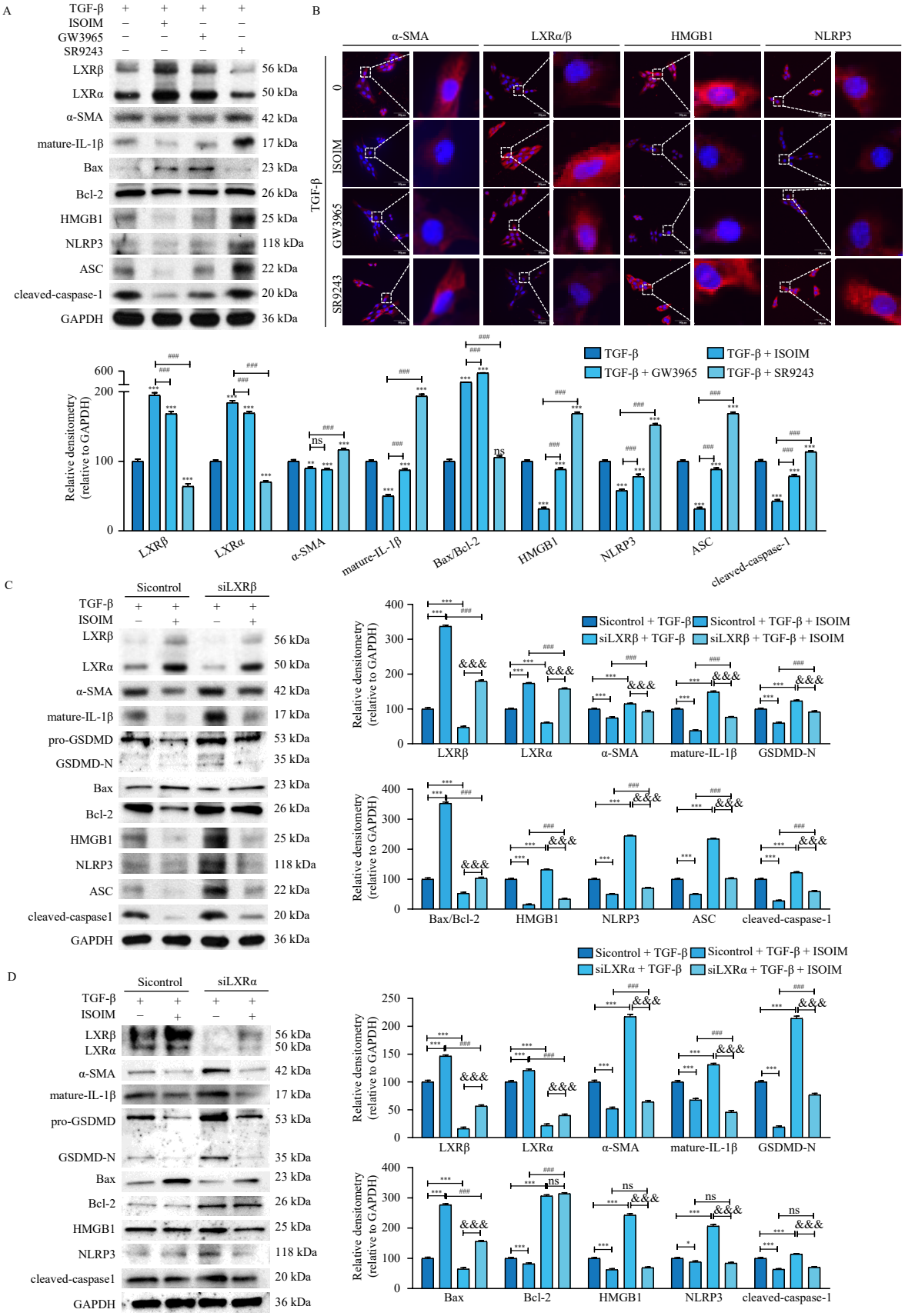


Fig. 6 LXRα/β-mediated HMGB1-NLRP3 axis might be indispensable for the anti-fibrotic effects of ISOIM. (A) Representative western blotting analysis of LXRβ, LXRα, α-SMA, mature-IL-1β, Bax, Bcl-2, HMGB1, NLRP3, ASC and cleaved-caspase-1 in TGF-β-stimulated HSCs. (B) Immunofluorescence staining of α-SMA, LXRα/β, HMGB1 and NLRP3 (600 × magnification, scale bar = 50 μm) in TGF-β-stimulated HSCs. (C) Representative western blotting analysis of LXRβ, LXRα, α-SMA, mature-IL-1β, GSDMD-N, Bax, Bcl-2, HMGB1, NLRP3, ASC and cleaved-caspase-1 in TGF-β-stimulated LX-2 with siLXRβ. (D) Representative western blotting analysis of LXRβ, LXRα, α-SMA, mature-IL-1β, GSDMD-N, Bax, Bcl-2, HMGB1, NLRP3 and cleaved-caspase-1 in TGF-β-stimulated LX-2 with siLXRα. Protein expressions were quantified relative to GAPDH as an internal control. Data were presented as mean ± SD (n = 3). Statistical significance was determined by one-way ANOVA with Tukey's post-hoc test. $^{*}P < 0.05$, $^{**}P < 0.01$, $^{***}P < 0.001$ *vs* TGF-β group or sicontrol + TGF-β group; $^{\#\#\#}P < 0.001$ *vs* TGF-β + ISOIM group or sicontrol + TGF-β + ISOIM group; $^{\&\&\&}P < 0.001$ *vs* siLXRβ or siLXRα + TGF-β group. ns, no significant difference.

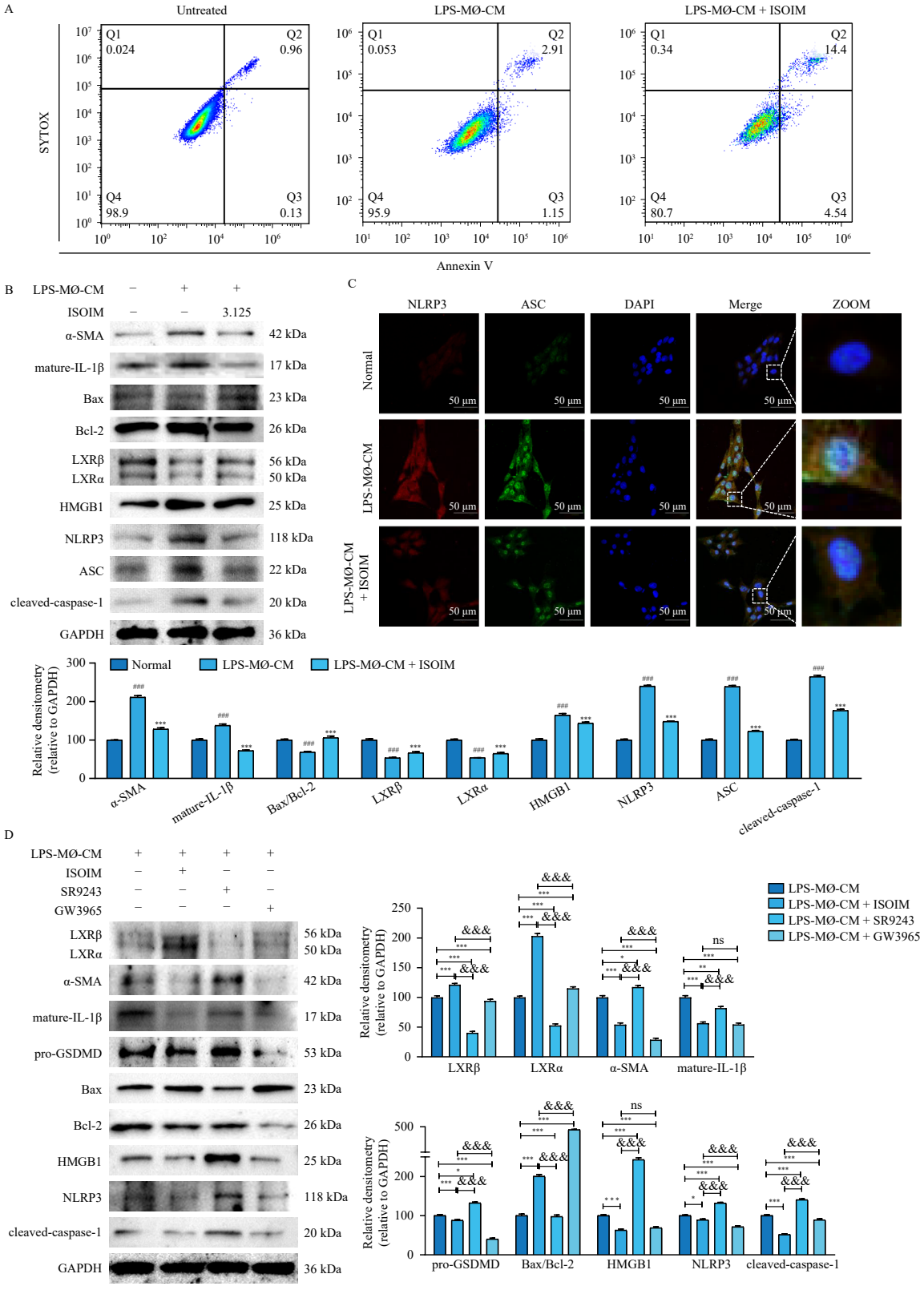


Fig. 7 ISOIM modulated the crosstalk of HSCs and macrophages *via* LXRα/β-mediated HMGB1-NLRP3 axis. (A) Flow cytometry of apoptotic staining in Annexin V-mCherry and SYTOX Green. (B) Representative western blotting analysis of α-SMA, mature-IL-1β, Bax, Bcl-2, LXRβ, LXRα, HMGB1, NLRP3, ASC and cleaved-caspase-1 in LPS-MØ-CM-stimulated LX-2. (C) Immunofluorescence staining of NLRP3 and ASC in LX-2 (600 × magnification, scale bar = 50 μm). (D) Representative western blotting analysis of α-SMA, mature-IL-1β, pro-GSDMD, Bax, Bcl-2, LXRβ, LXRα, HMGB1, NLRP3 and cleaved-caspase-1 in LPS-MØ-CM-stimulated LX-2 treated with ISOIM, SR9243 or GW3965. Protein expressions were quantified relative to GAPDH as an internal control. Data were presented as mean ± SD (n = 3). Statistical significance was determined by one-way ANOVA with Tukey's post-hoc test. $^{###}P < 0.001$ *vs* untreated LX-2 group; $^{*}P < 0.05$, $^{**}P < 0.01$, $^{***}P < 0.001$ *vs* LPS-MØ-CM group; $^{\&\&\&}P < 0.001$ *vs* LPS-MØ-CM + ISOIM group; ns, no significant difference.

These findings suggest that ISOIM may preferentially modulate the survival of activated HSCs while exhibiting relatively low hepatocyte toxicity, thereby supporting its potential value as an anti-fibrotic candidate.

In addition to apoptosis, NLRP3 inflammasome activation has been increasingly recognized as an important contributor to

hepatic inflammation and fibrosis [39]. In particular, NLRP3 inflammasome activation has been widely implicated in hepatocyte injury, macrophage activation, inflammatory amplification, and fibrogenic progression [40, 41]. In the present study, we found that ISOIM suppressed NLRP3 signaling in activated HSCs. However, the relationship between NLRP3 inflammasome signaling and apoptosis in activated HSCs remains insufficiently clarified, particularly in the context of pharmacological intervention. Notably, our results showed that NLRP3 signaling-related markers and apoptotic markers changed in opposite directions during fibrosis progression and ISOIM intervention. ISOIM enhanced caspase-3-dependent apoptotic signaling while reducing GSDMD-N-associated inflammatory signaling in activated HSCs. Specifically, pharmacological inhibition of NLRP3 by MCC950 reduced the levels of NLRP3 and GSDMD-N in activated HSCs, confirming the involvement of NLRP3 inflammasome signaling in this process. NLRP3 inhibition also increased caspase-3 activation and elevated the Bax/Bcl-2 ratio, suggesting a potential link between suppression of NLRP3 signaling and enhancement of apoptotic signaling in activated HSCs. Similar regulatory patterns were observed after ISOIM intervention, indicating that ISOIM may regulate the relationship between NLRP3 signaling and apoptotic signaling partly through inhibition of the NLRP3 inflammasome pathway. These findings suggest that suppression of NLRP3 signaling may be closely associated with the enhancement of apoptotic signaling in activated HSCs, and that ISOIM may exert its anti-fibrotic effects by suppressing NLRP3 inflammasome activation while enhancing apoptotic signaling.

Liver X receptors, including LXRα and LXRβ, are ligand-activated nuclear receptors with important roles in lipid metabolism, inflammatory regulation, and hepatic homeostasis [15-17]. Ginsenoside 25-OCH_3-PPD was reported to promote LXR activity and attenuate P2X7R-mediated NLRP3 inflammasome activation in TAA-induced hepatic fibrosis, while acanthoic acid ameliorated CCl_4-induced liver fibrosis through LXRα/β signaling and inhibited HSCs activation mainly through LXRβ activation [42, 43]. Despite these findings, the potential reciprocal regulation between LXRα and LXRβ in activated HSCs remains insufficiently understood. In the present study, ISOIM increased both LXRα and LXRβ expressions in fibrotic liver tissues and activated HSCs, and its effects were similar to those of the LXR agonist GW3965. Notably, LXRα knockdown reduced not only LXRα but also LXRβ expression, whereas LXRβ knockdown similarly decreased LXRα expression, suggesting a coordinated regulatory relationship between these two LXR isoforms in activated HSCs. Moreover, ISOIM restored LXRα/β expression and subsequently modulated HMGB1/NLRP3 signaling. These findings suggest that ISOIM might exert its anti-fibrotic effects through regulation of LXRα/β signaling, thereby contributing to the control of HMGB1/NLRP3 signaling and enhancing the apoptosis of activated HSCs.

Inflammation and inflammatory signaling are also closely involved in hepatic fibrosis progression, and inflammatory communication within the hepatic microenvironment can further promote HSCs activation. Increasing pharmacological studies suggest that natural products and small molecules can suppress inflammatory injury by targeting macrophage activation or inflammatory signaling [44-47]. In addition, a recent study demonstrated that macrophage GHSR-Foxo1 signaling promoted CCl_4-induced liver fibrosis by enhancing inflammatory responses and TGF-β-mediated HSCs activation, highlighting the importance of crosstalk between macrophages and HSCs in fibrosis development [48]. These studies suggest that inflammatory cell-mediated responses and natural product-based anti-inflammatory regulation are closely related to the progression and intervention of fibrotic diseases. In the present study, we further explored crosstalk between macrophages and HSCs using LPS-MØ-CM. Our results showed that macrophage-derived inflammatory stimulation promoted LX-2 activation and enhanced HMGB1/NLRP3 signaling. ISOIM attenuated these changes through activation of LXRα/β signaling, with effects similar to those of GW3965, thereby suppressing HMGB1/NLRP3 inflammatory signaling while enhancing activated LX-2 apoptosis. These findings suggest that ISOIM may interfere with macrophage-driven inflammatory and fibrogenic communication within the hepatic microenvironment *via* the LXRα/β-mediated HMGB1/NLRP3 signaling.

However, several limitations should be considered, including the limited evidence regarding the cell type-specific cytotoxicity, *in vivo* metabolism, and clinical translational potential of ISOIM. Future studies are needed to clarify the metabolism, bioavailability, and safety profile of ISOIM, as well as to validate its anti-fibrotic efficacy in hepatic fibrosis and related liver injury.

5. Conclusion

Taken together, the present study demonstrated that ISOIM attenuated hepatic fibrosis by reducing ECM accumulation, suppressing inflammatory responses, and promoting apoptotic signaling in activated HSCs. Mechanistically, ISOIM exerted these effects through LXRα/β-mediated regulation of the HMGB1/NLRP3 signaling. ISOIM also modulated crosstalk between macrophages and HSCs, thereby contributing to the improvement of the inflammatory hepatic microenvironment during fibrogenesis. These findings suggest that ISOIM has promising anti-fibrotic potential and provide a mechanistic foundation for its further development as a natural compound targeting hepatic fibrosis.

Funding

This work was supported by National Natural Science Foundation of China (Nos. 82560813, 81973555), Jilin Provincial Department of science and technology (No. 20250205012GH), and Natural Science Foundation of Jilin Province (No. YDZJ202501ZYTS270).

Declaration of competing interest

These authors have no conflict of interest to declare.

References

1 Pei Q, Yi Q, Tang L. Liver fibrosis resolution: from molecular mechanisms to therapeutic opportunities. *Int J Mol Sci*. 2023;24(11):9671. https://doi.org/10.3390/ijms24119671.
2 Jiang Y, Hou L, Dou J, et al. Sesamol as a potential candidate for the treatment of hepatic fibrosis, based on its regulation of FXR/LXR axis-mediated inhibition of autophagy through crosstalk between hepatic cells and macrophage. *Phytomedicine*. 2024;123:155145. https://doi.org/10.1016/j.phymed.2023.155145.
3 Zhao T, Zhong G, Wang Y, et al. Pregnane X receptor activation in liver macrophages protects against endotoxin-induced liver injury. *Adv Sci (Weinh)*. 2024;11(19):e2308771. https://doi.org/10.1002/advs.202308771.
4 Zhang N, Yao H, Zhang Z, et al. Ongoing involvers and promising therapeutic targets of hepatic fibrosis: the hepatic immune microenvironment. *Front Immunol*. 2023;14:1131588. https://doi.org/10.3389/fimmu.2023.1131588.
5 Friedman SL, Pinzani M. Hepatic fibrosis 2022: unmet needs and a blueprint for the future. *Hepatology*. 2022;75(2):473-488. https://doi.org/10.1002/hep.32285.
6 Liu L, Li B, Zhang Y, et al. MFAP4 deficiency attenuates liver fibrosis by regulating hepatic stellate cell fate through inhibition of the FAK/PI3K/NFκB signaling pathway. *Cell Mol Gastroenterol Hepatol*. 2025;19(10):101548. https://doi.org/10.1016/j.jcmgh.2025.101548.
7 Wang L, Huang Y, Chen J, et al. Dynamic crosstalk between HSCs and liver microenvironment: multicellular interactions in the regulation of liver fibrosis. *Front Cell Dev Biol*. 2025;13:1635763. https://doi.org/10.3389/fcell.2025.1635763.
8 Ge X, Desert R, Magdaleno F, et al. Redox-sensitive high-mobility group box-1 isoforms contribute to liver fibrosis progression and resolution in mice. *J Hepatol*. 2024;80(3):482-494. https://doi.org/10.1016/j.jhep.2023.11.005.
9 Ma X, Qiu J, Zou S, et al. The role of macrophages in liver fibrosis: composition, heterogeneity, and therapeutic strategies. *Front Immunol*. 2024;15:1494250. https://doi.org/10.3389/fimmu.2024.1494250.
10 Zhu L, Tong H, Ren C, et al. Inflammation unleashed: the role of pyroptosis in chronic liver diseases. *Int Immunopharmacol*. 2024;141:113006. https://doi.

org/10.1016/j.intimp.2024.113006.
11 Tseng HF, Chao HN, Lin CH, et al. Danshensu attenuates palmitic acid-induced activation of hepatic stellate cells by regulating pyroptosis. *Int J Med Sci*. 2025;22(8):1865-1874. https://doi.org/10.7150/ijms.107564.
12 Dou JY, Liu SH, Guo J, et al. Dietary supplementation of pterostilbene, a major component in small berries, prevents alcohol-induced liver injury associated with lipid accumulation and inflammation. *Food Funct*. 2024;15(22):11206-11219. https://doi.org/10.1039/d4fo03898c.
13 Dou JY, Cui ZY, Xuan MY, et al. Diallyl disulfide, the bioactive component of Allium species, ameliorates pulmonary fibrosis by mediating the crosstalk of farnesoid X receptor and yes-associated protein 1 signaling pathway. *Phytother Res*. 2024;38(8):4009-4021. https://doi.org/10.1002/ptr.8268.
14 Cai L, Yin M, Peng S, et al. RXRα modulates hepatic stellate cell activation and liver fibrosis by targeting CaMKKβ-AMPKα axis. *Acta Pharm Sin B*. 2025;15(7):3611-3631. https://doi.org/10.1016/j.apsb.2025.05.023.
15 Lockhart SM, Muso M, Zvetkova I, et al. Damaging mutations in liver X receptor-α are hepatotoxic and implicate cholesterol sensing in liver health. *Nat Metab*. 2024;6(10):1922-1938. https://doi.org/10.1038/s42255-024-01126-4.
16 Bousquet D, Nader E, Connes P, et al. Liver X receptor agonist upregulates LPCAT3 in human aortic endothelial cells. *Front Physiol*. 2024;15:1388404. https://doi.org/10.3389/fphys.2024.1388404.
17 Fang X, Zhang Y, Wang J, et al. Innate immune cell LXR-β deficiency exacerbates hepatic injury and fibrosis in murine models of primary sclerosing cholangitis. *Liver Res*. 2025;9(3):239-248. https://doi.org/10.1016/j.livres.2025.09.001.
18 Jiang C, Ding W, Hu Y, et al. Liver X receptor activation alleviates hepatic ischemia-reperfusion injury in diabetes by inhibiting NF-κB-NLRP3 activation. *Immun Inflamm Dis*. 2025;13(8):e70243. https://doi.org/10.1002/iid3.70243.
19 Clark AT, Russo-Savage L, Ashton LA, et al. A mutation in LXRα uncovers a role for cholesterol sensing in limiting metabolic dysfunction-associated steatohepatitis. *Nat Commun*. 2025;16(1):1102. https://doi.org/10.1038/s41467-025-56565-8.
20 Lu X, Yuan ZY, Yan XJ, et al. Effects of *Angelica dahurica* on obesity and fatty liver in mice. *Chin J Nat Med*. 2016;14(9):641-652. https://doi.org/10.1016/s1875-5364(16)30076-0.
21 Gao C, Hu ZH, Cui ZY, et al. *Angelica dahurica* extract and its effective component bergapten alleviated hepatic fibrosis by activating FXR signaling pathway. *J Nat Med*. 2024;78(2):427-438. https://doi.org/10.1007/s11418-024-01780-8.
22 Zhang J, Zhang Z, Cui T, et al. Prophylactic isoimperatorin protects against LPS-ALI *via* mTOR-dependent control of inflammation, oxidative stress and ferroptosis markers. *J Ethnopharmacol*. 2026;358:120998. https://doi.org/10.1016/j.jep.2025.120998.
23 Chen L, Yang H, Yu C, et al. High hepatic exposure of furanocoumarins in Radix *Angelica dahuricae* is associated with transporter mediated active uptake. *J Ethnopharmacol*. 2018;212:74-85. https://doi.org/10.1016/j.jep.2017.10.014.
24 Tang SY, Wang H, Zhang W, et al. Notopterygium forbesii boiss extract and its active constituents increase reactive species and heme oxygenase-1 in human fetal hepatocytes: mechanisms of action. *Chem Res Toxicol*. 2008;21(12):2414-2423. https://doi.org/10.1021/tx800301f.
25 Ko HJ, Park SY, Sim DY, et al. Apoptotic effect of Isoimpertorin *via* inhibition of c-Myc and SIRT1 signaling axis. *Int J Mol Sci*. 2024;25(8):4248. https://doi.org/10.3390/ijms25084248.
26 Kumar D, Bhat ZA, Kumar V, et al. Coumarins from *Angelica archangelica* Linn. and their effects on anxiety-like behavior. *Prog Neuropsychopharmacol Biol Psychiatry*. 2013;40:180-186. https://doi.org/10.1016/j.pnpbp.2012.08.004.
27 Fuster-Martínez I, Calatayud S. The current landscape of antifibrotic therapy across different organs: a systematic approach. *Pharmacol Res*. 2024;205:107245. https://doi.org/10.1016/j.phrs.2024.107245.
28 Steinberg GR, Carpentier AC, Wang D. MASH: the nexus of metabolism, inflammation, and fibrosis. *J Clin Invest*. 2025;135(18):e186420. https://doi.org/10.1172/jci186420.
29 Taru V, Szabo G, Mehal W, et al. Inflammasomes in chronic liver disease: hepatic injury, fibrosis progression and systemic inflammation. *J Hepatol*. 2024;81(5):895-910. https://doi.org/10.1016/j.jhep.2024.06.016.
30 Zhu C, Liu Z, Liu H, et al. Hepatocyte cuproptosis promotes the progression of hepatic fibrosis: emerging a potential therapeutic target. *Int Immunopharmacol*. 2026;170:116092. https://doi.org/10.1016/j.intimp.2025.116092.
31 Li T, Huo Y, Ji H, et al. A multifunctional L-arginine-linked melanin nanozyme for theranostic applications in liver fibrosis: non-invasive dual-modal imaging and reactive oxygen species scavenging for pyroptosis suppression. *J Colloid Interface Sci*. 2026;702(Pt 1):138872. https://doi.org/10.1016/j.jcis.2025.138872.
32 Iredale JP, Benyon RC, Pickering J, et al. Mechanisms of spontaneous resolution of rat liver fibrosis: hepatic stellate cell apoptosis and reduced hepatic expression of metalloproteinase inhibitors. *J Clin Invest*. 1998;102(3):538-549. https://doi.org/10.1172/jci1018.
33 Issa R, Williams E, Trim N, et al. Apoptosis of hepatic stellate cells: involvement in resolution of biliary fibrosis and regulation by soluble growth factors. *Gut*. 2001;48(4):548-557. https://doi.org/10.1136/gut.48.4.548.
34 Wang Y, Gao J, Zhang D, et al. New insights into the antifibrotic effects of sorafenib on hepatic stellate cells and liver fibrosis. *J Hepatol*. 2010;53(1):132-144. https://doi.org/10.1016/j.jhep.2010.02.027.
35 Su TH, Shiau CW, Jao P, et al. Sorafenib and its derivative SC-1 exhibit antifibrotic effects through signal transducer and activator of transcription 3 inhibition. *Proc Natl Acad Sci U S A*. 2015;112(23):7243-7248. https://doi.org/10.1073/pnas.1507499112.
36 Zhang J, Luan ZL, Huo XK, et al. Direct targeting of sEH with alisol B alleviated the apoptosis, inflammation, and oxidative stress in cisplatin-induced acute kidney injury. *Int J Biol Sci*. 2023;19(1):294-310. https://doi.org/10.7150/ijbs.78097.
37 Sun Z, Liang C, Zhao Y, et al. aHSCs-targeted bimetallic nanozymes and luteolin-loaded liposomes: synergistic reversal of liver fibrosis *via* antioxidant, cellular senescence, and cellular apoptotic mechanisms. *Mater Today Bio*. 2025;34:102201. https://doi.org/10.1016/j.mtbio.2025.102201.
38 Gayed M, Boraie N, El Achy S, et al. Mannosylated fenretinide loaded solid lipid nanoparticles alleviate liver fibrosis. *J Drug Deliv Sci Technol*. 2025;114:107417. https://doi.org/10.1016/j.jddst.2025.107417.
39 Xiao Y, Zhao C, Tai Y, et al. STING mediates hepatocyte pyroptosis in liver fibrosis by Epigenetically activating the NLRP3 inflammasome. *Redox Biol*. 2023;62:102691. https://doi.org/10.1016/j.redox.2023.102691.
40 Chen H, Zhou Y, Hao HP, et al. Emerging mechanisms of non-alcoholic steatohepatitis and novel drug therapies . *Chin J Nat Med*. 2024;22(8):724-745. https://doi.org/10.1016/S1875-5364(24)60690-4.
41 Bai T, Guo HL, Wang F, et al. Gut microbiota and HMGB1/NLRP3/GSDMD inflammasome-dependent pyroptosis: mechanisms by physcion ameliorates alcoholic liver fibrosis. *Front Pharmacol*. 2025;16:1532590. https://doi.org/10.3389/fphar.2025.1532590.
42 Han X, Song J, Lian LH, et al. Ginsenoside 25-OCH$_3$-PPD promotes activity of LXRs to ameliorate P2X7R-mediated NLRP3 inflammasome in the development of hepatic fibrosis. *J Agric Food Chem*. 2018;66(27):7023-7035. https://doi.org/10.1021/acs.jafc.8b01982.
43 Bai T, Yao YL, Jin XJ, et al. Acanthoic acid, a diterpene in *Acanthopanax koreanum*, ameliorates the development of liver fibrosis *via* LXRs signals. *Chem Biol Interact*. 2014;218:63-70. https://doi.org/10.1016/j.cbi.2014.04.016.
44 Zhang J, Yan J, Dong H, et al. Dimeric sesquiterpenoids with anti-inflammatory activities from Inula britannica. *Chin J Nat Med*. 2025;23(8):961-971. https://doi.org/10.1016/s1875-5364(25)60931-9.
45 Sun CP, Zhou JJ, Yu ZL, et al. Kurarinone alleviated Parkinson's disease *via* stabilization of epoxyeicosatrienoic acids in animal model. *Proc Natl Acad Sci U S A*. 2022;119(9):e2118818119. https://doi.org/10.1073/pnas.2118818119.
46 Zhang J, Zhang HL, Xu XR, et al. Targeting PBK with small-molecule 1-O-acetyl-4R,6S-britannilactone for the treatment of neuroinflammation. *Proc Natl Acad Sci U S A*. 2025;122(29):e2502593122. https://doi.org/10.1073/pnas.2502593122.
47 Zhang J, Zhang M, Huo XK, et al. Macrophage inactivation by small molecule wedelolactone *via* targeting sEH for the treatment of LPS-induced acute lung injury. *ACS Cent Sci*. 2023;9(3):440-456. https://doi.org/10.1021/acscentsci.2c01424.
48 Kim DM, Pan Q, Liu Z, et al. GHSR-Foxo1 signaling in macrophages promotes liver fibrosis *via* inflammatory response and hepatic stellate cell activation. *Adv Sci (Weinh)*. 2025;12(33):e04223. https://doi.org/10.1002/advs.202504223.